JOURNAL OF VIROLOGY, Aug. 2011, p. 7603–7612 Vol. 85, No. 15
0022-538X/11/$12.00 doi:10.1128/JVI.00562-11

Mechanisms of Human Immunodeficiency Virus Type 2 RNA Packaging: Efficient *trans* Packaging and Selection of RNA Copackaging Partners▽

Na Ni,[1] Olga A. Nikolaitchik,[1] Kari A. Dilley,[1] Jianbo Chen,[1] Andrea Galli,[1] William Fu,[2] V. V. S. P. Prasad,[1] Roger G. Ptak,[2] Vinay K. Pathak,[1] and Wei-Shau Hu[1]*

HIV Drug Resistance Program, National Cancer Institute—Frederick, Frederick, Maryland 21702,[1] and Department of Infectious Disease Research, Southern Research Institute, Frederick, Maryland 21701[2]

Received 21 March 2011/Accepted 18 May 2011

Human immunodeficiency virus type 2 (HIV-2) has been reported to have a distinct RNA packaging mechanism, referred to as *cis* packaging, in which Gag proteins package the RNA from which they were translated. We examined the progeny generated from dually infected cell lines that contain two HIV-2 proviruses, one with a wild-type *gag*/*gag-pol* and the other with a mutant *gag* that cannot express functional Gag/Gag-Pol. Viral titers and RNA analyses revealed that mutant viral RNAs can be packaged at efficiencies comparable to that of viral RNA from which wild-type Gag/Gag-Pol is translated. These results do not support the *cis*-packaging hypothesis but instead indicate that *trans* packaging is the major mechanism of HIV-2 RNA packaging. To further characterize the mechanisms of HIV-2 RNA packaging, we visualized HIV-2 RNA in individual particles by using fluorescent protein-tagged RNA-binding proteins that specifically recognize stem-loop motifs in the viral genomes, an assay termed single virion analysis. These studies revealed that >90% of the HIV-2 particles contained viral RNAs and that RNAs derived from different viruses were copackaged frequently. Furthermore, the frequencies of heterozygous particles in the viral population could be altered by changing a 6-nucleotide palindromic sequence at the 5′-untranslated region of the HIV-2 genome. This finding indicates that selection of copackaging RNA partners occurs prior to encapsidation and that HIV-2 Gag proteins primarily package one dimeric RNA rather than two monomeric RNAs. Additionally, single virion analyses demonstrated a similar RNA distribution in viral particles regardless of whether both viruses had a functional *gag* or one of the viruses had a nonfunctional *gag*, providing further support for the *trans*-packaging hypothesis. Together, these results revealed mechanisms of HIV-2 RNA packaging that are, contrary to previous studies, in many respects surprisingly similar to those of HIV-1.

Human immunodeficiency virus type 2 (HIV-2) is one of the two human lentiviruses that can cause AIDS. Compared with the global distribution of HIV-1 infection, reported HIV-2 cases are far more limited and are found mostly in West Africa (37). Both HIV-1 and HIV-2 were introduced into the human population by zoonotic transmission of simian immunodeficiency viruses (SIVs). HIV-2 originated from SIVs that infect sooty mangaby (SIV_{sm}) (21, 24, 33, 47), whereas HIV-1 originated from SIVs that infect chimpanzee (SIV_{cpz}) and gorilla (SIV_{gor}) (20, 49). Most of the genome structures of HIV-1 and HIV-2 are similar, and they share approximately 55% nucleotide sequence identity. Although many aspects of HIV-1 and HIV-2 replication are similar, it is thought that they use very different mechanisms for encapsidation of their genomes into viral particles (27).

Retroviruses encapsidate RNA into their particles, and virally encoded reverse transcriptases convert viral RNA genomes into double-stranded DNA molecules, which integrate into the host genome and become proviruses. The host cell machinery transcribes proviruses to generate viral RNAs, which can be spliced or remain unspliced as full-length viral RNAs. Full-length viral RNAs have at least two functions: they serve as templates for the translation of the viral genes *gag*/*gag-pol* and they are packaged into particles to serve as viral genomes (5). The encapsidation of viral RNA into particles is mediated by at least two viral components: the viral Gag polyproteins and an RNA element known as the packaging signal in the full-length RNA. The full-length viral RNAs from different retroviruses appear to use distinct mechanisms to serve their two known functions. Actinomycin D was used to treat murine leukemia virus (MLV)-infected cells to decrease transcription of nascent RNA; this treatment resulted in the production of many "empty" MLV particles lacking full-length viral RNAs (34). This finding demonstrated that there are two pools of MLV RNA, one with a longer half-life that is used for translation of viral proteins and another pool with a shorter half-life that is used for encapsidation of viral genomes (34, 35). Currently, there is no evidence that HIV-1 full-length RNAs are divided into two pools; actinomycin D treatment of host cells did not generate "empty" particles but diminished the generation of HIV-1 particles (14). It has been shown that HIV-1 RNA does not need to be translated to be packaged (6); furthermore, RNAs are packaged at similar efficiencies regardless of whether they encode functional Gag (41). Therefore, it has been concluded that the major mechanism for HIV-1 packaging is *trans* packaging (41). In contrast, it has been proposed

* Corresponding author. Mailing address: HIV Drug Resistance Program, NCI—Frederick, P.O. Box B, Building 535, Room 336, Frederick, MD 21702. Phone: (301) 846-1250. Fax: (301) 846-6013. E-mail: Wei-Shau.Hu@nih.gov.

▽ Published ahead of print on 25 May 2011.

that the major packaging mechanism for HIV-2 is *cis* packaging, i.e., Gag preferentially packages RNA from which it is translated (23, 27, 36). This conclusion was based on the observations that an element important for RNA encapsidation is located upstream of the splice donor site (23) and that HIV-2 RNA encoding truncated Gag was not rescued efficiently when a helper virus was added unless the RNAs encoded Gag, including a functional nucleocapsid domain (27). Therefore, the Gag-RNA interaction among various retroviruses appears to be quite different—from exclusively *trans*-acting, such as MLV, to mostly *cis*-acting, exemplified by HIV-2. The *cis*-packaging hypothesis also predicts dual negative selection forces for viruses containing *gag* mutations that cannot efficiently package viral RNA: in addition to their inability to produce infectious viruses, these mutant viral RNA genomes cannot be efficiently rescued by another virus.

Members of the *Retroviridae* are unique among viruses in that two complete copies of viral genetic material are packaged into one particle. Although it is known that the two packaged RNAs are dimeric in the particle, when and how RNA dimerization occurs remain unclear for some viruses. It has been shown that dimerized MLV RNA exposes RNA sequences that are high-affinity binding sites for Gag (15, 16); destroying these sites leads to drastic RNA packaging deficiencies (22). These results support the hypothesis that dimeric MLV RNAs are packaged into particles. In HIV-1, a 6-nucleotide (nt) palindromic sequence at the loop of stem-loop 1 of the viral RNA, termed the dimerization initiation signal (DIS), can affect the frequencies of RNA copackaging (7, 10, 38). RNA molecules with DIS sequences capable of forming intermolecular base pairing can be copackaged together more efficiently than RNAs that do not have compatible DIS sequences. Hence, HIV-1 RNA dimerization occurs prior to the encapsidation into viral particles (7). It is currently unknown whether HIV-2 Gag packages one dimeric or two monomeric RNAs. Furthermore, if translating RNAs are encapsidated, it is possible that ribosomes may disrupt the dimerized regions, thereby changing the dimeric/monomeric state of the packageble viral RNA.

Although it is unclear whether HIV-2 RNA is packaged as monomer or dimer, more than one RNA element has been suggested to play an important role in RNA dimerization. Similar to HIV-1, HIV-2 also has a proposed stem-loop structure (SL1) at the 5′-untranslated region (UTR) with a 6-nt palindrome at the loop location. Results from *in vitro* RNA dimerization studies have suggested that this 6-nt palindrome is important for the initiation of dimerization (13), although other *in vitro* studies suggest that another palindromic RNA element (*pal*) upstream of the 6-nt loop sequence is also important for dimerization (3, 29). Furthermore, cell culture experiments indicate that the 6-nt palindrome in SL1 is dispensable for RNA dimerization and virus replication (36); however, mutations in *pal* can have detrimental effects on RNA dimerization and virus replication (4, 30, 36). Thus, at this time, it is unclear which RNA element(s) is important for the RNA partner selection process if HIV-2 Gag packages dimeric RNA.

In this report, we used two different approaches to examine the mechanisms of HIV-2 RNA packaging. By examining virion RNA generated from cell lines containing HIV-2 proviruses, we found that HIV-2 RNA can be efficiently packaged in *trans*; without regard to whether one or both RNAs expressed a functional Gag. By tagging Gag and viral RNA with different fluorescent proteins, we were able to directly visualize HIV-2 RNA in each viral particle. Using the visualization assay, we found that the frequencies of heterozygous viral particle formation can be altered by changing the 6-nt palindrome in SL1, supporting the hypothesis that HIV-2 RNA dimerization occurs prior to genome encapsidation.

MATERIALS AND METHODS

Plasmid construction. In the descriptions below, the names of the plasmids start with a p, whereas the names of viruses derived from these plasmids do not. Plasmids pHIV2-H0G and pHIV2T600G have been previously described (8). Briefly, these vectors were derived from pROD12 and contain a 0.8-kb deletion in *env* and marker genes in the *nef* gene. Both of these constructs contain the *cis*-acting elements necessary for HIV-2 replication and express functional Gag/Gag-Pol, Tat, and Rev. In addition, pHIV2-H0G contains the mouse heat-stable antigen gene (*hsa*), whereas pHIV2-T600G contains the mouse Thy1.2 gene (*thy*); for clarity, these vectors are referred to as p2-WT-HSA and p2-WT-Thy, respectively. p2-WT-Thy was used to generate Gag truncation mutants p2*T-Hind3 and p2*T-Swa. In p2*T-Swa, a 21-bp sequence (TAGCCCGGGGTCAA TCAATCA) was inserted into the region encoding the N-terminal end of the nucleocapsid (NC) domain by introducing a premature stop codon after the seventh amino acid of NC. In p2*T-Hind3, a 4-bp sequence (AGCT) was inserted into the region encoding the capsid (CA) domain of Gag; this mutation generated a truncated Gag with matrix (MA) and 170 amino acids of CA. To generate p2*T-17, an additional substitution (AG to CT) was introduced in the MA region of *gag* in p2*T-Hind3, so that this construct contained two mutations and only expressed 16 amino acids of MA.

HIV-2 constructs used for RNA visualization are similar to pHIV2-H0G except that they contain deletions in *pol* and the insertion of an internal ribosomal entry site (IRES) *hsa* DNA fragment in *nef*. Unless specified otherwise, these constructs contain all of the *cis*-acting elements necessary for replication and express Gag, Tat, Rev, Vif, and Vpx. In all cases, two structurally similar constructs were generated: one expressing fluorescent protein-tagged Gag and the other expressing untagged Gag. For example, in p2-GagCeFP, *gag* is tagged with the cerulean fluorescent protein gene (*cefp*), whereas in p2-GagΔCeFP, a stop codon is present at the end of *gag* so that untagged Gag is expressed. To generate p2-GagCeFP-MSL and p2-GagΔCeFP-MSL, 24 copies of the stem-loop sequences recognized by MS2 coat proteins (19) were inserted into the *pol* genes of p2-GagCeFP and p2-GagΔCeFP, respectively. Similarly, 18 copies of the stem-loop sequences recognized by *Escherichia coli* BglG proteins (7) were inserted into p2-GagCeFP and p2-GagΔCeFP to generate p2-GagCeFP-BSL and p2-GagΔCeFP-BSL, respectively. Constructs with modified 6-nt palindromes in SL1 were generated by PCR-based mutagenesis and subcloning of an AatII-to-XhoI DNA fragment. Constructs p2-*17-GagCeFP-MSL and p2-*17-GagΔCeFP-MSL were generated by replacing an AatII-to-XhoI DNA fragment of p2-GagCeFP-MSL and p2-GagΔCeFP-MSL, respectively, with that of p2*T-17. The general structures of the plasmids were determined by restriction enzyme mapping, and portions of the plasmids generated by PCR were characterized by DNA sequencing to avoid inadvertent introduction of mutations during the amplification process.

Cell culture, transfection, infection, generation of producer cells, and flow cytometry. Human embryonic kidney cell line 293T and human T-cell line Hut78/CCR5 (HutR5) were maintained in Dulbecco's modified Eagle's medium and RPMI 1640 medium, respectively, which were supplemented with 10% fetal bovine serum, penicillin (50 U/ml), and streptomycin (50 μg/ml). Additionally, puromycin (1 μg/ml) and G418 (500 μg/ml) were added to the Hut/R5 medium. All cultured cells were maintained at 37°C in humidified incubators with 5% CO_2.

DNA transfection was performed using the calcium phosphate method (46) or FuGENE HD reagent (Roche). Virus generated from transfected cells was harvested, clarified through a 0.45-μm-pore-size filter, and either stored at −80°C or used directly for infection.

Producer cells containing 2-WT-HSA and *gag* mutants were generated by sequential infection of 293T cells and repeated cell sorting (45). Briefly, p2-WT-HSA and pHCMV-G, which express the vesicular stomatitis virus G protein (VSV-G) (50), were cotransfected into 293T cells, and the resulting virus was used to infect 293T cells at a low multiplicity of infection (MOI) of 0.05 to 0.1.

Infected HSA$^+$ cells were sorted and infected with *gag* mutant viruses at a low MOI. Virus stocks containing *gag* mutant genomes were generated by cotransfecting Gag mutant plasmid with an HIV-1 helper, CMVΔ8.2, which expresses HIV-1 proteins (40), and pHCMV-G. Doubly infected cells were enriched by cell sorting until >95% of the cells expressed HSA and Thy. To measure virus titers, the producer cells were transfected with the plasmid pIIINL(AD8)env, which encodes HIV-1 Env; viruses were harvested and used to infect Hut/R5 cells. Infected cells were stained with phycoerythrin-conjugated anti-HSA antibody (BD Biosciences) and allophycocyanin-conjugated anti-Thy-1.2 antibody (eBioscience) and fixed with 2% paraformaldehyde prior to flow cytometry analysis. Flow cytometry was performed using a FACSCalibur apparatus (BD Biosciences); cell sorting was performed on a FACSVantage SE system with the FACSDiVa digital option (BD Biosciences). Generally, all the cell lines were cell pools containing at least 10,000 independent infection events. Results obtained from flow cytometry were analyzed using FlowJo software (Tree Star).

RNA analysis. RNAs were isolated from producer cells and cell-free supernatants by using the QIAamp viral RNA minikit (Qiagen). A DNA sequencing-based method was used to determine the ratios of the wild-type versus mutant RNAs (32, 41). Briefly, RNA samples were used as templates to amplify a region of *gag* by revese transcription-PCR, and the amplified fragments were analyzed by DNA sequencing. The proportion of wild-type versus mutant *gag* was determined by peak heights of the sequencing signals and used to compare with the standard curve. Standard curves were generated by sequencing the PCR products amplified with mixtures of known ratios of wild-type and mutant plasmids. The *R* values of the standard curves were determined based on comparisons of the theoretical and measured ratios of the wild-type and mutant constructs. The *R* values of the standard curves in various experiments reported here were between 0.97 and 0.99.

Single virion analysis. HIV-2 constructs were transfected into 293T cells by using FuGENE HD reagent (Roche); supernatants were collected from transfected cells 18 h posttransfection, clarified through a 0.45-um-pore-size filter, and used immediately or stored at −80°C. The supernatants were mixed with 20 μl of Polybrene (1 mg/ml), placed on a glass-bottom dish (MatTek), and incubated for 2 h in a 37°C incubator with 5% CO_2 before image acquisition. Microscopy studies were performed by using an inverted Nikon eclipse Ti microscope, a 100× 1.40 numerical aperture oil objective, and an X-Cite 120 system (EXFO Photonic Solution Inc.) for illumination. Digital images were acquired by an ANDOR technology iXon camera and NIS element AR software (Nikon). The excitation and emission filter sets were 427/10 nm and 480/40 nm for CeFP, 504/12 nm and 542/27 nm for yellow fluorescent protein (YFP), and 577/25 nm and 632/60 nm for mCherry. Identification and colocalization of CeFP-labeled viral particles and RNA signals were performed using custom software developed with Matlab and DIP*image* as previously described (7). Merged images and pseudocolored images were generated with ImageJ software.

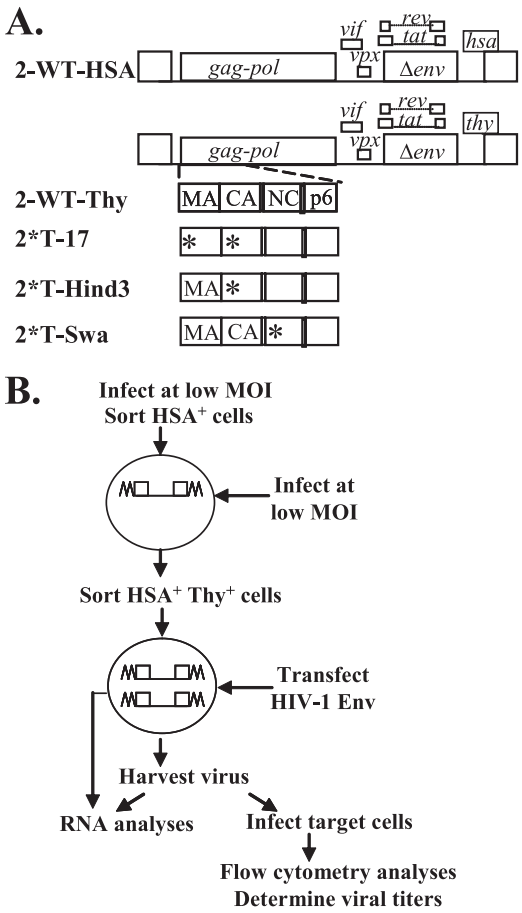

FIG. 1. Strategy to determine HIV-2 RNA packaging requirements. (A) General structures of modified HIV-2 genomes. (B) Protocol used to examine whether expression of a functional Gag is required for efficient RNA packaging. All HIV-2 genomes include a nonfunctional *gfp* in *nef*, which is not shown for simplicity. Asterisks indicate inactivating mutations.

RESULTS

Effects of the genes on HIV-2 RNA packaging efficiency. We developed a competition assay to determine whether HIV-2 RNA must express functional Gag proteins to be packaged efficiently. In this assay, virus-producing cells were generated that expressed two HIV-2 proviruses with similar general structures: one expressed wild-type Gag/Gag-Pol and the other could not express a functional Gag. We then compared the levels of RNA packaged into the particles and the viral titers of these two viruses.

We used HIV-2 vectors that contained near-full-length genomes with inactivating mutations in *vpr* and *env* (Fig. 1A); additionally, these vectors contained a marker gene followed by an IRES and an inactivated *gfp* in the *nef* region. Vector p2-WT-HSA and p2-WT-Thy encode wild-type Gag/Gag-Pol and expressed the marker gene *hsa* or *thy*, respectively. Vectors p2*T-17, p2*T-Hind3, and p2*T-Swa contain mutant *gag* and the marker gene *thy*. In p2*T-Swa, 21 nt was inserted into the 5′ end of the NC coding region, which generated an in-frame stop codon. Hence, this vector expressed a truncated Gag containing MA, CA, sp1, and 7 amino acids of NC; most of the NC (including the two conserved CCHC motifs), sp2, and p6 were deleted. In p2*T-Hind3, a frameshift mutation was introduced into the CA domain; as a result, this mutant expressed a truncated Gag with MA and 170 amino acids of CA. The frameshift mutation in p2*T-Hind3 was introduced downstream to the proposed internally initiated Gag translation start codon; therefore, both full-length and internally initiated Gag translation were truncated by this mutation. In p2*T-17, two mutations were introduced in *gag*, the aforementioned Hind3 mutation and a substitution (AG to CT) to generate a stop codon at the 17th amino acid in MA. As a result, 2*T-17 expresses a 16-amino-acid peptide of MA.

We generated producer cell lines containing a 2-WT-HSA and a *gag* mutant provirus by sequential infection and cell sorting (Fig. 1B). Briefly, 293T cells were infected at a low MOI with VSV-G-pseudotyped 2-WT-HSA virus; infected cells were enriched by cell sorting based on the expression of the HSA marker encoded by the virus. These enriched cells were infected at a low MOI by a second virus stock that had the *thy*-containing *gag* mutant genome pseudotyped with HIV-1 Gag/Gag-Pol and VSV-G. Based on the expression of HSA and Thy, doubly infected cells were enriched by cell sorting

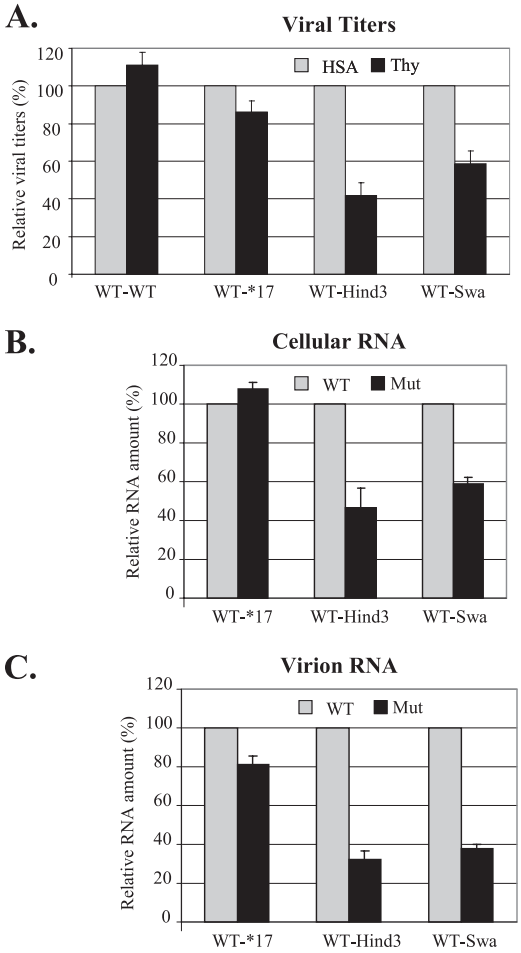

FIG. 2. Comparisons of viral titers (A), RNA expression levels (B), and virion RNA encapsidation (C) from cells containing a provirus with wild-type *gag* and a provirus with mutant *gag*. In all panels, values from 2-WT-HSA were set as 100%, and the values from mutant viruses are shown relative to the 2-WT-HSA values. Data shown are summarized from at least three independent experiments; error bars indicate standard deviations.

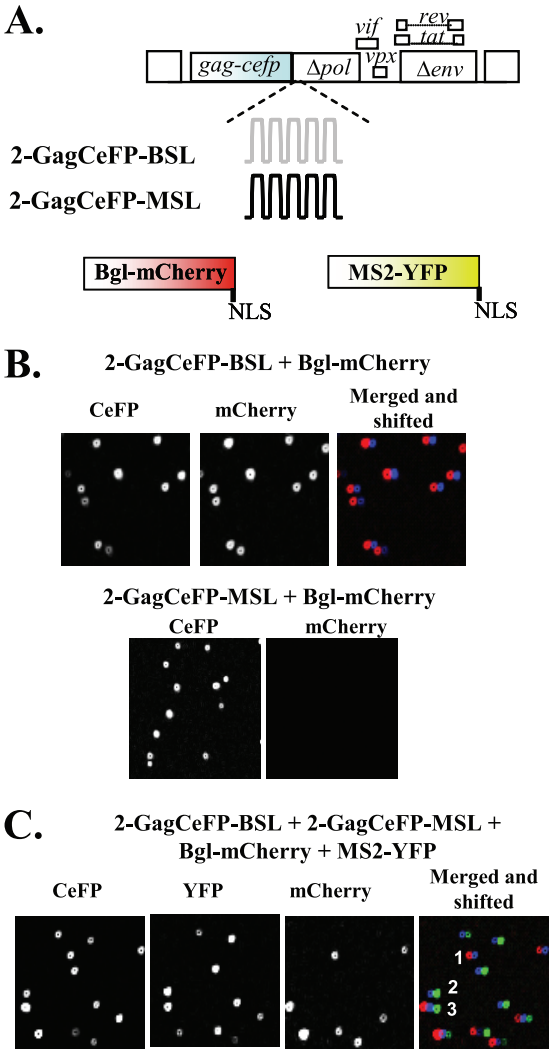

FIG. 3. Examination of HIV-2 RNA encapsidation by single virion analysis. (A) Modified HIV-2 genomes that contain stem-loop sequences and RNA-binding proteins tagged with fluorescent proteins. NLS, nuclear localization signal. (B) Representative images of particles from coexpressing Bgl-mCherry with either 2-GagCeFP-BSL or 2-GagCeFP-MSL. (C) Representative images of particles from coexpression of 2-GagCeFP-BSL, 2-GagCeFP-MSL, Bgl-mCherry, and MS2-YFP. CeFP particles indicated by numbers 1, 2, and 3 also showed mCherry, YFP, and mCherry plus YFP signals, respectively. All experiments were performed with coexpression of GagCeFP and untagged Gag; for simplicity, only the GagCeFP constructs are indicated.

until more than 95% of the cells in the final cell line expressed both markers. Thus, each cell line contained a large pool of dually infected cells generated from >10,000 infection events.

To examine the 2-WT-HSA and *gag* mutant virus titers, producer cells were transfected with pIIINL(AD8)env, a plasmid that expresses CCR5-tropic HIV-1 envelope. Viruses were harvested and used to infect the human T cell line Hut/R5, which was then stained with antibody and analyzed by flow cytometry. Wild-type and *gag* mutant virus titers were determined based on HSA and Thy expression. Results from four experiments are summarized in Fig. 2A; HSA titers were set as 100%, whereas Thy titers are shown relative to the HSA titer. The positive control was a cell line containing 2-WT-HSA and 2-WT-Thy (Fig. 2A; WT-WT); viruses harvested from WT-WT generated similar HSA and Thy titers. We then compared viral titers from producer cells containing 2-WT-HSA and a *gag* mutant virus. The 2*T-17 mutant generated titers similar to that of the wild-type virus (WT-*17), whereas the other two mutants, 2*T-Hind3 and 2*T-Swa, generated titers that were lower, ~40% and ~60%, respectively, than the 2-WT-HSA viral titers.

We then examined the relative expression of the wild-type and *gag* mutant proviruses in the producer cells and the viral RNA packaged into virions. Results summarized from at least three independent experiments are shown in Fig. 2B and C. Mutant 2*T-17 RNA was expressed and packaged at a level similar to that of the wild-type virus (Fig. 2B and C, WT-*17). Both 2*T-Hind3 and 2*T-Swa mutants were expressed at levels lower than, but within 2-fold of, the wild-type viral RNA (Fig. 2B, WT-Hind3 and WT-Swa); it is possible that mutations may have slight effects on RNA biogenesis or stability. Importantly,

TABLE 1. Single virion analyses of RNA detected in HIV-2 particles

Combination and expt	No. of CeFP particles analyzed	% of particles that were CFP$^+$ and:			RNA labeling efficiency[a] (%)
		YFP$^+$	mCherry$^+$	YFP$^+$ and mCherry$^+$	
2-BSL[b] + Bgl-mCherry					
Expt 1	3,139	0.2	92.9	0.0	92.9
Expt 2	1,697	0.0	92.1	0.0	92.1
Expt 3	1,115	0.0	96.5	0.0	96.5
2-BSL + MS2-YFP					
Expt 1	2,933	1.0	0.0	0.0	1.0
Expt 2	1,929	0.2	0.0	0.0	0.2
Expt 3	1,624	0.1	0.0	0.0	0.1
2-MSL + MS2-YFP					
Expt 1	1,457	87.2	0.0	0.0	87.2
Expt 2	686	89.7	0.0	0.0	89.7
Expt 3	702	87.7	0.0	0.0	87.7
2-MSL + Bgl-mCherry					
Expt 1	1,267	0.0	0.2	0.0	0.2
Expt 2	1,634	0.0	0.0	0.0	0.0
Expt 3	1,168	0.0	0.0	0.0	0.0
2-BSL + 2-MSL + Bgl-mCherry + MS2-YFP					
Expt 1	1,339	27.7	28.2	36.3	91.7
Expt 2	972	29.2	32.0	31.2	92.4
Expt 3	1,125	34.4	24.6	32.3	91.3
Expt 4	1,161	19.7	37.6	36.0	93.4
Expt 5	1,599	25.7	34.8	32.3	92.9
Expt 6	1,558	31.4	28.2	33.4	93.0
Expt 7	3,038	26.3	32.4	34.4	93.0
Expt 8	2,668	24.0	36.2	34.3	94.5

[a] Calculated by adding the values from the previous three columns.
[b] For simplicity, the "GagCeFP" portions of all the construct names were deleted; for example, 2-BSL is 2-GagCeFP-BSL.

the level of decrease in *gag* mutant RNA expression in the producer cells corresponded to the level of decrease in viral titers. Furthermore, comparing the ratios of the wild-type and mutant RNAs expressed in the producer cells and packaged in the viral particles showed that mutant RNA can be packaged efficiently into the particles (Fig. 2C, WT-Hind3 and WT-Swa). Taken together, the results of the viral titer and RNA analyses demonstrated that HIV-2 RNAs can be packaged efficiently into virions regardless of whether the RNA encodes a functional Gag.

Examining RNA packaging efficiency by visualizing HIV-2 RNA using single virion analysis. To better understand the mechanisms of HIV-2 RNA packaging, we directly visualized HIV-2 RNA in viral particles using microscopy by labeling Gag and RNAs with different fluorescent proteins. This strategy was previously used to examine HIV-1 RNA packaging (7). For this purpose, HIV-2 genomes were modified to express a Gag-CeFP fusion protein and contain the stem-loop sequences BSL or MSL, which are recognized by RNA binding proteins *E. coli* BglG antitermination protein (Bgl) or bacteriophage MS2 coat protein, respectively (Fig. 3A). These modified HIV-2 genomes contain all the *cis*-acting elements required for virus replication and express functional Vif, Vpx, Tat, and Rev; additionally, they contain an *hsa* gene in the *nef* gene position. For each Gag-CeFP-expressing construct, a structurally similar sister construct was generated to express wild-type Gag. In all experiments, both Gag-CeFP and Gag constructs were coexpressed to avoid potential distortion of viral particle morphology. For brevity, only the Gag-CeFP construct is illustrated in the figures and mentioned in the text. To analyze the RNA content in the viral particles, HIV-2 vectors expressing Gag-CeFP and their sister vectors expressing Gag were cotransfected into 293T cells along with plasmids expressing the RNA-binding proteins. Viral particles were harvested and visualized by fluorescence microscopy.

We first examined the viral RNA packaging efficiencies of HIV-2 particles by using viral RNA containing Bgl stem-loops, 2-GagCeFP-BSL (Fig. 3A), and tagged RNA-binding protein Bgl-mCherry. An example of the viral particle analyses is shown in the upper panels of Fig. 3B: the CeFP channel detected Gag signals and the mCherry channel detected the RNA signals; the merged and shifted panel shows the overlap images with the mCherry channel shifted 4 pixels to the left. The results of multiple experiments demonstrated that most of the CeFP particles also displayed mCherry signals (Table 1). To ensure that the RNA signal detected was specific, we also performed similar analyses of HIV-2 genomes containing MS2 stem-loops coexpressed with Bgl-mCherry, and we did not observe mCherry signals in the particles (Fig. 3B, lower panels, and Table 1). Together, these results indicate that most (>90%) of the HIV-2 particles contain viral RNAs and that HIV-2 encapsidation is an efficient process.

We also examined the incorporation of HIV-2 RNA containing the stem-loops recognized by MS2 coat proteins. Sim-

ilar to the results from the Bgl system, when viral RNA contained the corresponding stem-loops (MSL), most CeFP signals also had colocalized YFP signals, as the MS2 coat proteins were tagged with YFP; in contrast, coexpression of 2-Gag-CeFP-BSL RNA with MS2-YFP resulted in negligible YFP signals (Table 1). However, compared with Bgl-mediated RNA labeling, our detection of HIV-2 RNA using the MS2 system was slightly less efficient (Table 1).

Determination of the efficiencies of copackaging RNAs derived from different HIV-2 constructs. To probe whether RNAs derived from different HIV-2 constructs are copackaged into the same particles efficiently, we coexpressed HIV-2 containing either Bgl or MS2 stem-loops along with the two tagged RNA-binding proteins. A set of representative images is shown in Fig. 3C; Gag signals were detected in the CeFP channel, whereas the RNA signals were detected in either the YFP or the mCherry channel. An image of signals detected in all three channels is also shown (merged and shifted), with signals detected in the YFP and mCherry channels shifted to the right and left by 4 pixels, respectively. Three CeFP particles (Fig. 3C, numbers 1, 2, and 3) displayed mCherry, YFP, and YFP plus mCherry signals, indicating that these particles contained RNAs with BSL, MSL, and both MSL and BSL RNAs, respectively. Results from multiple independent experiments are shown in Table 1. Theoretically, when two viruses (virus A and virus B) express RNA at the same level and RNA packaging is completely random, we would expect 25%, 50%, and 25% of the progeny particles to contain two copies of A RNA, one copy of A RNA plus one copy of B RNA, and two copies of B RNA, respectively (Hardy-Weinberg equilibrium). In our experiments, we observed that heterozygous viruses were formed quite frequently (~34% of the viral population) but less frequently than expected for a random distribution.

Examination of whether HIV-2 RNAs are packaged as dimers or monomers. We envision two possible mechanisms by which HIV-2 packages two RNAs into the virus particle. Viral RNAs may be packaged as dimers, and RNA partner selection occurs prior to encapsidation. In this scenario, altering the viral dimerization signals may affect the RNA partner selection process, thereby changing the ratio of heterozygous particles in the viral population. Alternatively, two monomeric RNAs may be packaged into one particle, and RNA dimerization occurs after encapsidation. In this case, changing the dimerization signals should not affect the ratio of heterozygous particles. To test these two hypotheses, we examined the effects of changing the dimerization signal on the ratios of heterozygous particle formation. More than one sequence motif has been proposed to be important for HIV-2 RNA dimerization (29, 36); among them is a 6-nt palindrome in the loop region of SL1 (Fig. 4A) that is parallel to the DIS of HIV-1 both in location and in the palindromic nature of the sequence. We hypothesized that this palindrome is important for selecting the RNA partner, and we examined the effects of changing the loop sequences on HIV-2 RNA packaging and dimerization. The sequence of this palindrome in the molecular clone ROD12 is GGTACC; we changed this sequence in the HIV-2 constructs to GCGCGC (3GC), the DIS sequence for HIV-1 subtype B variants (Fig. 4B). Using single virion analysis, we found that efficient RNA encapsidation occurred in viral particles derived from HIV-2 constructs containing the 3GC sequences, 2-3GC-GagCeFP-MSL and

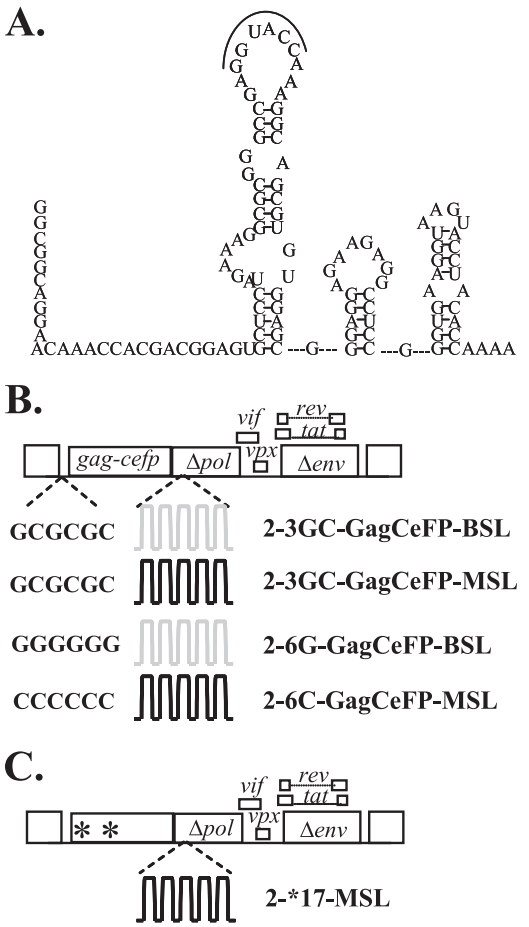

FIG. 4. HIV-2 5′-UTR and modified HIV-2 genomes. (A) Proposed structure of a portion of the HIV-2 5′ UTR (36). (B) General structures of the modified HIV-2 genomes with altered loop sequences in SL1. (C) Modified HIV-2 genomes containing two inactivating mutations in *gag* to terminate translations.

2-3GC-GagCeFP-BSL (Table 2). Furthermore, when these two constructs with 3GC were coexpressed, heterozygous particles were formed at frequencies similar to those of two HIV-2 constructs containing the wild-type sequences (Table 2). These results indicate that replacing the GGTACC sequence with GCG CGCx did not cause defects in RNA encapsidation or copackaging efficiency. We then examined the distributions of RNA in particles when the two HIV-2 constructs contained noncomplementary palindromes by coexpressing 2-GagCeFP-BSL and 2-3GC-GagCeFP-MSL. Our results showed that the heterozygous particle ratio in the viral population was reduced to 13% (Table 2), about 2.5-fold lower than the heterozygous ratio when the RNAs from the two viruses had the same palindromes.

To further test the impact of the palindromic sequence on the ratio of heterozygous particles in the viral population, we generated HIV-2 constructs containing either GGGGGG (6G) or CCCCCC (6C) instead of the GGTACC wild-type sequence. Efficient RNA encapsidation was observed in particles generated by 2-6G-GagCeFP-BSL or 2-6C-GagCeFP-MSL (Table 3). We then examined the viral population generated from coexpressing 2-6G-GagCeFP-BSL and 2-6C-GagCeFP-MSL; our results showed that the proportions of the heterozy-

TABLE 2. Single virion analysis of HIV-2 particles from genomes containing altered 6-nt palindromes in SL1

Combination and expt	No. of CeFP particles analyzed	% of particles that were CeFP$^+$ and:			RNA labeling efficiency[a] (%)
		YFP$^+$	mCherry$^+$	YFP$^+$ and mCherry$^+$	
2-3GC-BSL[b] + Bgl-mCherry					
Expt 1	2,218	0.0	95.8	0.0	95.8
Expt 2	3,908	0.0	92.7	0.0	92.7
Expt 3	4,123	0.0	93.6	0.3	93.9
2-3GC-BSL + MS2-YFP					
Expt 1	2,775	0.1	0.0	0.0	0.1
Expt 2	3,912	1.2	0.0	0.0	1.2
Expt 3	3,021	0.4	0.0	0.0	0.4
2-3GC-MSL + MS2-YFP					
Expt 1	1,125	90.1	0.0	0.0	90.1
Expt 2	411	89.1	0.0	0.0	89.1
Expt 3	799	89.9	0.0	0.0	89.9
2-3GC-MSL + Bgl-mCherry					
Expt 1	2,657	0.0	0.0	0.0	0.0
Expt 2	1,920	0.1	0.0	0.0	0.1
Expt 3	1,178	0.0	0.1	0.0	0.1
2-3GC-BSL + 2-3GC-MSL + Bgl-mCherry + MS2-YFP					
Expt 1	1,247	23.4	33.4	35.9	92.8
Expt 2	1,492	22.7	39.7	31.1	93.5
Expt 3	1,710	34.4	22.7	35.6	92.7
Expt 4	2,711	38.4	19.3	36.9	94.5
2-BSL + 2-3GC-MSL + Bgl-mCherry + MS2-YFP					
Expt 1	804	40.0	37.3	15.3	92.7
Expt 2	1,034	45.5	30.6	15.9	91.9
Expt 3	850	49.5	32.5	11.6	93.7
Expt 4	562	40.6	41.1	10.5	92.2

[a] Calculated by adding the values from the previous three columns.
[b] For simplicity, the "GagCeFP" portions of all the construct names were deleted; for example, 2-3GC-BSL is 2-3GC-GagCeFP-BSL.

gous particles were approximately 57% of the viral population (Table 3), which is approximately 1.6 times higher than that of viruses with GGTACC sequences.

Taken together, these results demonstrate that the ratios of heterozygous particles can be altered significantly by changing a palindromic sequence; therefore, RNA partner selection occurs prior to most of the viral RNA packaging. Additionally, the 6-nt palindromic sequence at the loop of SL1 plays an important role in RNA partner selection.

Probing the mechanisms of encapsidation of HIV-2 RNA encoding nonfunctional Gag. As most of the HIV-2 RNAs are encapsidated as dimers, it can be argued that Gag proteins recognize the RNAs encoding functional Gag, and RNA-RNA association allows the encapsidation of the genomes encoding nonfunctional Gag. This modified *cis*-packaging hypothesis predicts that most of the mutant RNAs encapsidated should be in heterozygous particles. Alternatively, if both wild-type and mutant RNAs are encapsidated by the same mechanism, then the homozygous and heterozygous particle distribution should be similar to those generated by the two wild-type viruses. To distinguish between these two hypotheses, we modified 2-GagCeFP-MSL and generated a *gag* mutant construct that contained the inactivating mutations described for the *17 mutant, with two stop codons in the MA- and CA-encoding regions (Fig. 4C). As expected, these constructs did not generate viral particles (data not shown). We then examined the viral population generated by coexpressing 2-GagCeFP-BSL and 2-*17-GagCeFP-MSL. We found that the ratio of the heterozygous particles was approximately 29% (Table 4); more importantly, there were plenty of CeFP particles with only YFP labeling, indicating that most of these particles had only the RNA containing the *17 mutations. We also analyzed the viral population generated by coexpressing 2-3GC-GagCeFP-BSL and 2-*17-GagCeFP-MSL (Table 4), and we observed homozygous and heterozygous ratios similar to those from two comparable viruses, both of which contain a functional *gag* gene. Therefore, the 2-*17 mutant RNAs were packaged by Gag recognition and not by association with the wild-type *gag*-containing RNA.

DISCUSSION

HIV-2 has often been referred to as the representative retrovirus that encapsidates its genome through a *cis*-acting mechanism (5). The development of HIV-2 vectors that do not encode Gag in *cis* argues that HIV-2 Gag is capable of packaging RNA in *trans* (2, 43). However, the efficiencies of these events have not been determined and, therefore, cannot ad-

TABLE 3. Single virion analysis of homozygous and heterozygous particles with 6G and 6C DIS mutants

Combination and expt	No. of CeFP particles analyzed	% of particles that were CeFP$^+$ and:			RNA labeling efficiency[a] (%)
		YFP$^+$	mCherry$^+$	YFP$^+$ and mCherry$^+$	
2-6G-BSL[b] + Bgl-mCherry					
Expt 1	2,488	0.0	92.9	0.0	92.9
Expt 2	2,071	0.0	92.8	0.0	92.8
Expt 3	1,405	0.1	93.1	0.0	93.2
Expt 4	3,267	0.0	91.0	0.0	91.0
2-6G-BSL + MS2-YFP					
Expt 1	1,659	1.1	0.0	0.0	1.1
Expt 2	3,890	0.9	0.0	0.0	0.9
Expt 3	2,810	0.5	0.0	0.0	0.5
Expt 4	4,037	0.7	0.0	0.0	0.7
2-6C-MSL + MS2-YFP					
Expt 1	826	91.8	0.0	0.0	91.8
Expt 2	873	90.0	0.0	0.0	90.0
Expt 3	1,060	91.4	0.0	0.0	91.4
Expt 4	824	91.3	0.0	0.1	91.4
Expt 5	1,474	91.3	0.0	0.0	91.3
2-6C-MSL + Bgl-mCherry					
Expt 1	1,401	0.0	0.0	0.0	0.0
Expt 2	1,671	0.0	0.0	0.0	0.1
Expt 3	1,734	0.0	0.0	0.0	0.0
2-6G-BSL + 2-6C-MSL + Bgl-mCherry + MS2-YFP					
Expt 1	773	12.9	21.5	57.8	92.2
Expt 2	1,336	17.5	18.9	57.0	93.5
Expt 3	887	14.2	20.6	57.2	92.0
Expt 4	1,638	18.7	18.4	54.9	92.1

[a] Calculated by adding the values from the previous three columns.
[b] For simplicity, the "GagCeFP" portions of all the construct names were deleted; for example, 2-6G-BSL is 2-6G-GagCeFP-BSL.

dress whether the major mechanism of HIV-2 RNA packaging is *cis*- or *trans*-acting. In this report, we examined the packaging of structurally similar, near-full-length HIV-2 genomes and found that HIV-2 Gag can efficiently package HIV-2 RNA regardless of whether the RNA encodes functional Gag. One of the mutants, 2*T-17, expresses only 16 amino acids of the N terminus of Gag; however, its RNA is packaged at a level similar to that of the wild-type RNA. Furthermore, using the newly developed single virion analysis, we directly visualized the RNA contents of the viral particles. These studies revealed that *gag* mutant RNAs were packaged as homodimers efficiently by Gag proteins that were translated from another RNA. Together, these results support the conclusion that *trans* packaging is the major mechanism by which HIV-2 packages its RNA.

Does *cis* packaging occur in HIV-2? Given the observation that viral RNAs that do not encode functional Gag can be efficiently packaged, it is difficult to generate data to directly prove the occurrence of *cis* packaging, as one has to demonstrate the Gag proteins in the particle came from one of the

TABLE 4. Single virion analysis of particles derived from coexpression of two HIV-2 constructs, one of which does not express Gag

Combination and expt	No. of CeFP particles analyzed	% of particles that were CeFP$^+$ and:			RNA labeling efficiency[a] (%)
		YFP$^+$	mCherry$^+$	YFP$^+$ and mCherry$^+$	
2-BSL[b] + 2-*17-MSL + Bgl-mCherry + MS2-YFP					
Expt 1	1,291	27.3	36.0	27.8	91.2
Expt 2	1,959	14.1	50.3	30.4	94.8
Expt 3	4,701	12.2	50.0	28.8	91.0
2-3GC-BSL + 2-*17-MSL + Bgl-mCherry + MS2-YFP					
Expt 1	1,780	39.1	41.5	9.7	90.2
Expt 2	5,177	20.7	59.7	13.2	93.5
Expt 3	5,432	17.5	59.1	15.7	92.3

[a] Calculated by adding the values from the previous three columns.
[b] For simplicity, the "GagCeFP" portions of all the construct names were deleted; for example, 2-BSL is 2-GagCeFP-BSL.

two RNA molecules that were packaged. As a result, we cannot address at this time whether *cis* packaging does occur at some frequency.

Most packaging studies analyze RNA isolated from a viral population and cannot address the frequency by which "wild-type" virus packages its genome. By directly visualizing RNA in the viral particles, we observed that >90% of the HIV-2 viral particles contained RNAs; this feature is similar to the efficient RNA encapsidation in HIV-1 (7). It is quite possible that high-efficiency encapsidation is a common feature of lentiviruses.

Whether RNA dimerization occurs prior to encapsidation has been a long-standing question in retrovirology. The results from various studies suggest that the Gag proteins from both MLV and HIV-1 recognize one dimer rather than two monomers (7, 10, 16, 22, 38). In the current report, we examined the RNA contents of HIV-2 particles directly and found that the ratios of the heterozygous particles could be altered significantly by changing a 6-nt sequence in SL1 of the 5′-UTR. If viral RNA were packaged as two monomers, the ratio of heterozygous particles in the viral population would not be altered by changing this sequence. The fact that only 13% of the particles are heterozygous when the two viruses contain noncomplementary 6-nt sequences supports the hypothesis that HIV-2 Gag proteins package one dimeric RNA most of the time.

The role of the 6-nt palindromic sequence in RNA dimerization has been the subject of controversy; although *in vitro* experiments have shown that this 6-nt RNA motif is important for RNA dimerization, cell culture-based experiments have demonstrated that destroying the 6-nt palindromic sequence does not affect RNA dimerization (3, 4, 13, 29–31, 36). In our report, we show that this palindromic sequence is a major element responsible for the copackaged viral RNA selection. In this respect, the 6-nt palindromic sequence in HIV-2 is very similar to the DIS in HIV-1, which also plays a critical role in RNA partner selection, although mutant viruses without this palindromic sequence still package RNA efficiently and have dimeric RNA in the particles (39, 42) (Table 3). HIV-1 variants with different DIS sequences have evolved; there are two major sequences and multiple minor sequences (26, 48). Variation in the DIS sequences represents a barrier for copackaging of RNA from different variants and affects their recombination rates (9, 10). We have also examined the 6-nt sequence in HIV-2 by using the available sequences in the Los Alamos HIV sequence database, and we did not observe variation in these sequences. Despite the important role played by the DIS, there are currently undefined RNA elements in HIV-1 that are important for RNA dimerization (9). Therefore, we speculate that, similar to HIV-1, there are other *cis*-acting elements in the HIV-2 genome that are important for RNA dimerization.

In this report, we observe that when both viruses have the wild-type 6-nt palindromes, ~34% of the HIV-2 particles have two different RNAs (Table 1). As described in the Results section, if the two parent viruses are expressed at similar levels and the RNA packaging is random, 50% of the viral particles generated are expected to be heterozygous. As ~90% of the particles have RNA signals (Table 1), approximately 38% of the particles with RNA signals are heterozygous, which is approximately 75% of the expected value from random assortment. Using similar strategies, we examined the RNA copackaging in HIV-1, and we observed that ~45% of the viral particles are heterozygous or ~48% of the particles with RNA signals have two different RNAs, a frequency higher than that of the HIV-2 heterozygous viral particles. These results raised the possibility that HIV-2 RNA copackaging is not completely random. It has been suggested that MLV RNA dimerization is not random, although the frequency of MLV heterozygous particle formation has not yet been determined. Based on results of genetic studies, it was estimated that only ~8% of the MLV viral population can generate genotypically different progenies, even though recombination occurs frequently (1, 11, 12, 25); biochemical assays also showed that RNA heterodimers seem to form less frequently in MLV than in HIV-1 (17). RNA derived from stably cotransfected MLV vectors dimerizes more frequently than RNAs from sequentially transfected MLV vectors, indicating that the integration sites can affect recombination potential and suggesting that MLV RNA dimerizes at an early stage during RNA biogenesis (18, 28, 44). Our measurement of the HIV-2 heterozygous particle frequency (~34%) is much higher than the estimation of that of MLV (~8%) and is closer to the measured HIV-1 heterozygous rate (~45%). It is possible that the HIV-2 copackaging is not completely random, and there is a small bias toward homodimerization. Although we do not know the mechanism(s) that causes this putative bias, one can speculate that perhaps HIV-2 RNA dimerizes at a stage slightly earlier than that of HIV-1, causing this slight bias to homodimerization. Alternatively, it is possible that technical issues resulted in the measured ~34%; the RNA labeling efficiency of our HIV-2 constructs containing MS2 stem-loops was slightly lower than that of HIV-1 (7), which resulted in the difference of the measured heterozygous rate.

It has been proposed that HIV-1 and HIV-2 have very different RNA packaging mechanisms (27). In this report, we have shown that there are similarities among many aspects of the RNA packaging in these two viruses. First, both viruses can efficiently package full-length viral RNA that does not encode functional Gag; hence, *trans* packaging is the major RNA encapsidation mechanism. Second, the Gag proteins of both viruses mainly package dimeric RNA. Lastly, a 6-nt palindromic sequence at the 5′-UTR is used by both viruses to perform RNA partner selection. These unexpected findings reveal insights into HIV-2 RNA packaging mechanisms and the conserved features between these two human pathogens.

ACKNOWLEDGMENTS

We thank Anne Arthur for her expert editorial help and Eric Freed and Gisela Heidecker-Fanning for discussions.

This research was supported in part by the Intramural Research Program of the NIH National Cancer Institute Center for Cancer Research and by IATAP funding from NIH.

REFERENCES

1. **Anderson, J. A., E. H. Bowman, and W. S. Hu.** 1998. Retroviral recombination rates do not increase linearly with marker distance and are limited by the size of the recombining subpopulation. J. Virol. **72:**1195–1202.
2. **Arya, S. K., M. Zamani, and P. Kundra.** 1998. Human immunodeficiency virus type 2 lentivirus vectors for gene transfer: expression and potential for helper virus-free packaging. Hum. Gene Ther. **9:**1371–1380.
3. **Baig, T. T., J. M. Lanchy, and J. S. Lodmell.** 2007. HIV-2 RNA dimerization is regulated by intramolecular interactions in vitro. RNA **13:**1341–1354.
4. **Baig, T. T., J. M. Lanchy, and J. S. Lodmell.** 2009. Randomization and in

vivo selection reveal a GGRG motif essential for packaging human immunodeficiency virus type 2 RNA. J. Virol. **83:**802–810.
5. **Butsch, M., and K. Boris-Lawrie.** 2002. Destiny of unspliced retroviral RNA: ribosome and/or virion? J. Virol. **76:**3089–3094.
6. **Butsch, M., and K. Boris-Lawrie.** 2000. Translation is not required To generate virion precursor RNA in human immunodeficiency virus type 1-infected T cells. J. Virol. **74:**11531–11537.
7. **Chen, J., et al.** 2009. High efficiency of HIV-1 genomic RNA packaging and heterozygote formation revealed by single virion analysis. Proc. Natl. Acad. Sci. U. S. A. **106:**13535–13540.
8. **Chen, J., D. Powell, and W. S. Hu.** 2006. High frequency of genetic recombination is a common feature of primate lentivirus replication. J. Virol. **80:**9651–9658.
9. **Chin, M. P., J. Chen, O. A. Nikolaitchik, and W. S. Hu.** 2007. Molecular determinants of HIV-1 intersubtype recombination potential. Virology **363:** 437–446.
10. **Chin, M. P., T. D. Rhodes, J. Chen, W. Fu, and W. S. Hu.** 2005. Identification of a major restriction in HIV-1 intersubtype recombination. Proc. Natl. Acad. Sci. U. S. A. **102:**9002–9007.
11. **Delviks, K. A., W. S. Hu, and V. K. Pathak.** 1997. Psi- vectors: murine leukemia virus-based self-inactivating and self-activating retroviral vectors. J. Virol. **71:**6218–6224.
12. **Delviks, K. A., and V. K. Pathak.** 1999. Effect of distance between homologous sequences and 3′ homology on the frequency of retroviral reverse transcriptase template switching. J. Virol. **73:**7923–7932.
13. **Dirac, A. M., H. Huthoff, J. Kjems, and B. Berkhout.** 2001. The dimer initiation site hairpin mediates dimerization of the human immunodeficiency virus, type 2 RNA genome. J. Biol. Chem. **276:**32345–32352.
14. **Dorman, N., and A. Lever.** 2000. Comparison of viral genomic RNA sorting mechanisms in human immunodeficiency virus type 1 (HIV-1), HIV-2, and Moloney murine leukemia virus. J. Virol. **74:**11413–11417.
15. **D'Souza, V., A. Dey, D. Habib, and M. F. Summers.** 2004. NMR structure of the 101-nucleotide core encapsidation signal of the Moloney murine leukemia virus. J. Mol. Biol. **337:**427–442.
16. **D'Souza, V., and M. F. Summers.** 2004. Structural basis for packaging the dimeric genome of Moloney murine leukaemia virus. Nature **431:**586–590.
17. **Flynn, J. A., W. An, S. R. King, and A. Telesnitsky.** 2004. Nonrandom dimerization of murine leukemia virus genomic RNAs. J. Virol. **78:**12129–12139.
18. **Flynn, J. A., and A. Telesnitsky.** 2006. Two distinct Moloney murine leukemia virus RNAs produced from a single locus dimerize at random. Virology **344:**391–400.
19. **Fusco, D., et al.** 2003. Single mRNA molecules demonstrate probabilistic movement in living mammalian cells. Curr. Biol. **13:**161–167.
20. **Gao, F., et al.** 1999. Origin of HIV-1 in the chimpanzee Pan troglodytes troglodytes. Nature **397:**436–441.
21. **Gao, F., et al.** 1992. Human infection by genetically diverse SIV_{SM}-related HIV-2 in west Africa. Nature **358:**495–499.
22. **Gherghe, C., et al.** 2010. Definition of a high-affinity Gag recognition structure mediating packaging of a retroviral RNA genome. Proc. Natl. Acad. Sci. U. S. A. **107:**19248–19253.
23. **Griffin, S. D., J. F. Allen, and A. M. Lever.** 2001. The major human immunodeficiency virus type 2 (HIV-2) packaging signal is present on all HIV-2 RNA species: cotranslational RNA encapsidation and limitation of Gag protein confer specificity. J. Virol. **75:**12058–12069.
24. **Hirsch, V. M., R. A. Olmsted, M. Murphey-Corb, R. H. Purcell, and P. R. Johnson.** 1989. An African primate lentivirus (SIVsm) closely related to HIV-2. Nature **339:**389–392.
25. **Hu, W. S., E. H. Bowman, K. A. Delviks, and V. K. Pathak.** 1997. Homologous recombination occurs in a distinct retroviral subpopulation and exhibits high negative interference. J. Virol. **71:**6028–6036.
26. **Hussein, I. T., et al.** 2010. Delineation of the preferences and requirements of the human immunodeficiency virus type 1 dimerization initiation signal by using an in vivo cell-based selection approach. J. Virol. **84:**6866–6875.
27. **Kaye, J. F., and A. M. Lever.** 1999. Human immunodeficiency virus types 1 and 2 differ in the predominant mechanism used for selection of genomic RNA for encapsidation. J. Virol. **73:**3023–3031.
28. **Kharytonchyk, S. A., A. I. Kireyeva, A. B. Osipovich, and I. K. Fomin.** 2005. Evidence for preferential copackaging of Moloney murine leukemia virus genomic RNAs transcribed in the same chromosomal site. Retrovirology **2:**3.
29. **Lanchy, J. M., and J. S. Lodmell.** 2002. Alternate usage of two dimerization initiation sites in HIV-2 viral RNA in vitro. J. Mol. Biol. **319:**637–648.
30. **Lanchy, J. M., and J. S. Lodmell.** 2007. An extended stem-loop 1 is necessary for human immunodeficiency virus type 2 replication and affects genomic RNA encapsidation. J. Virol. **81:**3285–3292.
31. **Lanchy, J. M., C. A. Rentz, J. D. Ivanovitch, and J. S. Lodmell.** 2003. Elements located upstream and downstream of the major splice donor site influence the ability of HIV-2 leader RNA to dimerize in vitro. Biochemistry **42:**2634–2642.
32. **Leitner, T., et al.** 1993. Analysis of heterogeneous viral populations by direct DNA sequencing. Biotechniques **15:**120–127.
33. **Lemey, P., et al.** 2003. Tracing the origin and history of the HIV-2 epidemic. Proc. Natl. Acad. Sci. U. S. A. **100:**6588–6592.
34. **Levin, J. G., P. M. Grimley, J. M. Ramseur, and I. K. Berezesky.** 1974. Deficiency of 60 to 70S RNA in murine leukemia virus particles assembled in cells treated with actinomycin D. J. Virol. **14:**152–161.
35. **Levin, J. G., and M. J. Rosenak.** 1976. Synthesis of murine leukemia virus proteins associated with virions assembled in actinomycin D-treated cells: evidence for persistence of viral messenger RNA. Proc. Natl. Acad. Sci. U. S. A. **73:**1154–1158.
36. **L'Hernault, A., J. S. Greatorex, R. A. Crowther, and A. M. Lever.** 2007. Dimerisation of HIV-2 genomic RNA is linked to efficient RNA packaging, normal particle maturation and viral infectivity. Retrovirology **4:**90.
37. **McCutchan, F. E.** 2006. Global epidemiology of HIV. J. Med. Virol. **78**(Suppl. 1)**:**S7–S12.
38. **Moore, M. D., et al.** 2007. Dimer initiation signal of human immunodeficiency virus type 1: its role in partner selection during RNA copackaging and its effects on recombination. J. Virol. **81:**4002–4011.
39. **Moore, M. D., and W. S. Hu.** 2009. HIV-1 RNA dimerization: it takes two to tango. AIDS Rev. **11:**91–102.
40. **Naldini, L., et al.** 1996. In vivo gene delivery and stable transduction of nondividing cells by a lentiviral vector. Science **272:**263–267.
41. **Nikolaitchik, O., T. D. Rhodes, D. Ott, and W. S. Hu.** 2006. Effects of mutations in the human immunodeficiency virus type 1 Gag gene on RNA packaging and recombination. J. Virol. **80:**4691–4697.
42. **Paillart, J. C., M. Shehu-Xhilaga, R. Marquet, and J. Mak.** 2004. Dimerization of retroviral RNA genomes: an inseparable pair. Nat. Rev. Microbiol. **2:**461–472.
43. **Poeschla, E., et al.** 1998. Identification of a human immunodeficiency virus type 2 (HIV-2) encapsidation determinant and transduction of nondividing human cells by HIV-2-based lentivirus vectors. J. Virol. **72:**6527–6536.
44. **Rasmussen, S. V., and F. S. Pedersen.** 2006. Co-localization of gammaretroviral RNAs at their transcription site favours co-packaging. J. Gen. Virol. **87:**2279–2289.
45. **Rhodes, T. D., O. Nikolaitchik, J. Chen, D. Powell, and W. S. Hu.** 2005. Genetic recombination of human immunodeficiency virus type 1 in one round of viral replication: effects of genetic distance, target cells, accessory genes, and lack of high negative interference in crossover events. J. Virol. **79:**1666–1677.
46. **Sambrook, J., E. F. Fritsch, and T. Maniatis.** 1989. Molecular cloning: a laboratory manual, 2nd ed. Cold Spring Harbor Laboratory Press, Cold Spring Harbor, NY.
47. **Santiago, M. L., et al.** 2005. Simian immunodeficiency virus infection in free-ranging sooty mangabeys (Cercocebus atys atys) from the Tai Forest, Cote d'Ivoire: implications for the origin of epidemic human immunodeficiency virus type 2. J. Virol. **79:**12515–12527.
48. **St. Louis, D. C., et al.** 1998. Infectious molecular clones with the nonhomologous dimer initiation sequences found in different subtypes of human immunodeficiency virus type 1 can recombine and initiate a spreading infection in vitro. J. Virol. **72:**3991–3998.
49. **Van Heuverswyn, F., et al.** 2006. Human immunodeficiency viruses: SIV infection in wild gorillas. Nature **444:**164.
50. **Yee, J. K., et al.** 1994. A general method for the generation of high-titer, pantropic retroviral vectors: highly efficient infection of primary hepatocytes. Proc. Natl. Acad. Sci. U. S. A. **91:**9564–9568.